Fluxoid Quantization and Field-Induced Depairing in a Hollow Superconducting Microcylinder*

R. P. GROFF† AND R. D. PARKS
Department of Physics and Astronomy, University of Rochester, Rochester, New York

(Received 24 June 1968)

Little and Parks demonstrated that the superconducting transition temperature T_c of a multiply connected superconductor is periodic in a magnetic field with a periodicity of $hc/2e$. However, there were certain anomalous features of the early experiments, such as an unexplained temperature dependence of the amplitude of the ΔT_c oscillations and an unexplained nonoscillatory magnetic field background superposed on the oscillatory field dependence of T_c. By repeating the experiment under more controlled conditions, we have eliminated the problems which led to the anomalous features of the early results. Isothermal resistance-versus-magnetic-field measurements were made on Sn and Al cylinders of various diameters in the range 1–5 μ. From these measurements detailed phase diagrams (T_c-versus-H curves) were constructed which are in excellent agreement with the predictions of the linearized Ginzburg-Landau theory. The present type of experiment is shown to be suitable for studying depairing due to kinetic-energy effects associated with the drift motion of Cooper pairs. The results are discussed within the framework of the pair-breaking theory of Abrikosov and Gor'kov, which has been adapted to treat the present problem.

I. INTRODUCTION

THE concept of fluxoid (or flux) quantization has received considerable attention since the original prediction by London[1] and subsequent experimental verification by Deaver and Fairbank[2] and by Doll and Näbauer[3] (see, e.g., Ref. 4 and the quoted bibliography). The fluxoid Φ is defined by

$$\Phi=\iint_{S'}\mathbf{H}\cdot d\mathbf{S}+c\oint_{C'}\Lambda\mathbf{J}\cdot d\mathbf{l}=n(hc/2e), \qquad (1)$$

where S' is a surface containing a hole and bounded by a curve C', H is the applied magnetic field, c is the speed of light, J is the supercurrent density, $\Lambda=m/n_se^2$ is the London parameter (m being the effective electronic mass, e the electronic charge, and n_s the number of superconducting electrons), h is Planck's constant, and n is an integer. In a bulk superconductor, essentially all of the current flows on the surface (or edges) within a layer of thickness $\lambda(T)$ [typically $\sim$1000 Å $(1-T/T_c)^{-1/2}$] called the weak field penetration depth. For the case of a sufficiently thick multiply connected superconductor (e.g., a thick ring or hollow cylinder) at $T\ll T_c$, one can choose the curve C' to lie wholly within the superconductor where $J=0$. Thus the second term in Eq. (1) vanishes and one is left with the result that the flux threading the hole is quantized in units of $hc/2e\equiv\phi_0$.[5,6] This was the experimental situation of Doll and Näbauer and of Deaver and Fairbank, who verified that the flux in the hole was indeed quantized in units of $hc/2e$. The other extreme of an infinitely thin hollow cylinder in an axial magnetic field with $T_c-T\ll T_c$ was first considered by Little and Parks.[7,8] For this case $\lambda\gg d$, the thickness of the cylinder walls, and one can no longer choose the curve C' in a region where $J=0$. Thus the flux in the hole is no longer strictly quantized because the integral around C' contributes to Φ.[4,9,10] In fact for this case, fields from screening currents [those currents contributing to the second integral in Eq. (1)] are negligible and the flux inside the hole is approximately equal to the applied field. Any quantum effects must therefore arise from the second term in Eq. (1). Using the Ginzburg-Landau theory[11] and Eq. (1), Tinkham[9] derived the following expression for the variation of T_c with axial magnetic field in vanishingly thin, hollow cylindrical superconductors of radius R:

$$\Delta T_c/T_c=(n\phi_0-\pi R^2H)^2/8\pi^2R^2\lambda^2(0)H_{cb}^2(0), \qquad (2)$$

where $\lambda(0)$ and $H_{cb}(0)$ are the penetration depth and critical field at $T=0$°K, respectively.

Little and Parks[7,8] found the transition temperature of thin hollow cylinders of various superconductors to be periodic with period $hc/2e$ in the applied magnetic flux threading the cylinder. However, presumably because of sample inhomogeniety and/or nonuniformity of cylinder diameter, little information beyond the period of the oscillations [e.g., the verification of the functional form of Eq. (2) or a quantitative measurement of $(\Delta T_c)_{\max}$] could be extracted from the experiments.

Another well-known effect present in thin (simply connected) superconducting films is the increase in the

* Work supported in part by the U.S. Army Research Office (Durham) under Grant No. DA-31-124-ARO-D-G844.

† Present address: Central Research Department, E. I. du Pont de Nemours and Company, Experimental Station, Wilmington, Del.

[1] F. London, *Superfluids* (John Wiley & Sons, Inc., New York, 1950), p. 152.

[2] B. S. Deaver and W. M. Fairbank, Phys. Rev. Letters **7**, 43 (1961).

[3] R. Doll and M. Näbauer, Phys. Rev. Letters **7**, 50 (1961).

[4] D. H. Douglass, Jr., Phys. Rev. **132**, 513 (1963).

[5] The original prediction of London was that the flux should be quantized in units of hc/e. However, within the framework of the BCS theory the charge carriers are not single electrons, but pairs of electrons with charge $2e$ and mass $2m$.

[6] J. Bardeen, L. N. Cooper, and J. R. Schrieffer, Phys. Rev. **108**, 1175 (1957).

[7] W. A. Little and R. D. Parks, Phys. Rev. Letters **9**, 9 (1962).

[8] R. D. Parks and W. A. Little, Phys. Rev. **133**, A97 (1964).

[9] M. Tinkham, Phys. Rev. **129**, 2413 (1963); Rev. Mod. Phys. **36**, 268 (1964).

[10] C. Delmasso and E. Pagiola, Nuovo Cimento **35**, 811 (1965).

[11] V. L. Ginzburg and L. D. Landau, Zh. Eksperim. i Teor. Fiz. **20**, 1064 (1950).

parallel critical field $H_{||}(T)$ relative to $H_{cb}(T)$, the thermodynamic critical field for bulk superconductors. The following expression[12] for $H_{||}(T)$ can be found from the Ginzburg-Landau equations:

$$H_{||}(T)=(2\sqrt{6})[\lambda(T)/d]H_{cb}(T). \quad (3)$$

This expression is valid for films of thickness

$$d<(\sqrt{5})\lambda(T), \quad (4)$$

which is just the condition for the phase transition from the normal to the superconducting state to be second order.

We report here the results of new experiments carried out under more controlled experimental conditions, from which we have constructed the critical-field-versus-temperature phase diagrams for thin-walled hollow Al and Sn cylinders of the Little-Parks type. These results are compared with the solutions of the Ginzburg-Landau equations, which we show reduce to a combination of Eqs. (2) and (3) in the appropriate limit. A brief review of the salient features of the properties of the solutions of the Ginzburg-Landau equations for small hollow cylinders will be followed by a presentation of the experimental work. In addition, we shall discuss the significance of the present work in terms of its relevance to the problem of depairing[13] in superconductors.

II. PROPERTIES OF SOLUTIONS OF GINZBURG-LANDAU EQUATIONS FOR A HOLLOW CYLINDER

For the case of a hollow cylinder undergoing a second-order phase transition, the following expression can be derived which relates the critical axial magnetic field and the temperature:

$$\frac{\kappa^2}{\lambda^2}=\frac{1}{R_m^2}\left[(h-n)^2+h^2\left(\frac{d}{2R_m}\right)^2+n^2\left(\frac{d}{2R_m}\right)^2\left\{\frac{1}{3}+\frac{1}{5}\left(\frac{d}{2R_m}\right)^2+O\left[\left(\frac{d}{2R_m}\right)^4\right]\right\}\right], \quad (5)$$

where we have introduced the reduced field variable $h=\pi R_m^2 H/\phi_0$, R_m is the mean radius of the cylinder, and n is an integer which is free to change so as to keep the Gibbs free-energy difference ΔG between the normal and superconducting state of the cylinder maximized. [For this case, the minimum value of ΔG corresponds to the highest transition temperature; i.e., n is chosen so as to keep the transition temperature of the cylinder in Eq. (5) as large as possible for a given value of field.] A review of the boundary conditions and assumptions leading to Eq. (5) is presented in Appendix A. The penetration depth λ and Ginzburg-Landau coupling constant κ can be found from Eqs. (A3) and (A4), respectively. All terms involving the quantum number n and field appear on the right side of Eq. (5), while the temperature dependence is restricted to the left side only. Figure 1(a) is a plot of Eq. (5) for the ratio $d/2R_m=0.3$. For the extreme case $d/2R_m=0$, the local maxima in transition temperature all fall at the same value of temperature instead of successively lower values as in Fig. 1(a). The fields h_M corresponding to the local maxima in transition temperature can be found by solving Eq. (5) for h, subject to the condition $dh/dt=\infty$, which yields

$$h_M=\frac{n}{1+(d/2R_m)^2}. \quad (6)$$

Using Eq. (6), Eq. (5) can be put into the form

$$\frac{\kappa^2}{\lambda^2}=\frac{1}{R_m^2}\left[(h-h_M)^2\left\{1+\left(\frac{d}{2R_m}\right)^2\right\}+\tfrac{1}{3}h_M^2\frac{d^2}{R_m^2}\left\{1+\frac{7}{5}\left(\frac{d}{2R_m}\right)^2+O\left[\left(\frac{d}{2R_m}\right)^4\right]\right\}\right]. \quad (7)$$

This procedure has the advantage of separating the terms which are periodic in field from those which are not. The envelope curve for the nonperiodic terms in Eq. (7) may be determined simply by setting $h=h_M$ in Eq. (7) and using Eqs. (A3) and (A4) for κ^2/λ^2, giving

$$H(T)_{\text{envelope}}=2\sqrt{6}[\lambda(T)/d]H_{cb}(T)\times\{1+(7/5)(d/2R_m)^2+\cdots\}^{1/2}, \quad (8)$$

which just reduces to the value for the critical field of a simply connected film [Eq. (3)] for sufficiently large R_m.

Similarly, the value of field for which the transition temperature is a local minimum is found by writing the right side of Eq. (5) or Eq. (7) as $f(h, n)$ and solving $f(h_m, n)=f(h_m, n-1)$ for h_m, giving

$$h_m=\tfrac{1}{2}(2n+1)[1+\tfrac{1}{3}(d/2R_m)^2+\cdots] \quad (9)$$

or

$$R_m^2=R^2[1+\tfrac{1}{3}(d/2R_m)^2+\cdots], \quad (10)$$

with

$$R^2=\phi_0/\pi(\Delta H)_{\min}, \quad (11)$$

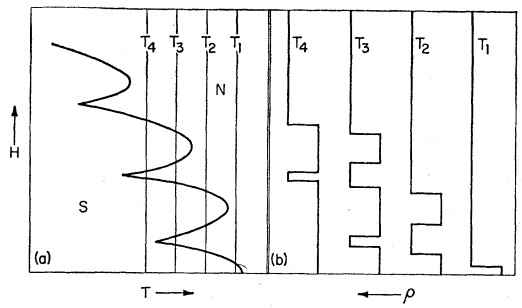

FIG. 1. (a) Phase diagram for cylinder with finite wall thickness $(d/2R)=0.3$ [from Eq. (12)]. (b) Expected resistivity-versus-magnetic-field curves for the four isotherms shown in Fig. 1(a).

[12] D. H. Douglass, Jr., Phys. Rev. **124**, 735 (1961).
[13] N. N. Bogoliubov, Zh. Eksperim. i Teor. Fiz. **34**, 58 (1958) [English transl.: Soviet Phys.—JETP **7**, 41 (1958)].

where $(\Delta H)_{\min}$ is the difference in field between two adjacent temperature minima. For all of the samples used in this study (see Secs. V and VI) the correction terms of order $(d/2R)^2$ and higher introduced a difference of less than 4% between R_m and R, i.e., $R_m-R<0.04R$. Inserting the standard temperature dependences[14] for κ^2/λ^2 and including terms to second order in $d/2R$, Eq. (7) becomes, for temperatures close to T_c,

$$\Delta t_c=\frac{\phi_0^2}{8\pi^2\lambda^2(0)H_{cb}^2(0)R^2}\left\{(h'-h_{M'})^2\left[1+\frac{4}{3}\left(\frac{d}{2R}\right)^2\right]+\tfrac{1}{3}h_{M'}{}^2\frac{d^2}{R^2}\right\}, \quad (12)$$

where $h'=\pi R^2H/\phi_0$, and

$$\Delta t_c=[T_c(h'=0)-T_c(h')]/T_c(h'=0).$$

The values of successive minima in T_c can easily be found from Eq. (12). However, as is the case with successive maxima in T_c, this quantity increases markedly with increasing field [see, for example, Fig. 1(a)], even for extremely small values of $d/2R$. For comparison with experiment it is convenient to divide Δt_c into terms which are periodic and aperiodic in field, i.e., $\Delta t_c=(\Delta t_c)_{\text{per}}+(\Delta t_c)_{\text{aper}}$. Then we obtain for the maxima of the periodic part [henceforth, $(\Delta t_c)_{\max\ \text{per}}\equiv(\Delta t_c)_{\max}$],

$$(\Delta t_c)_{\max}=\frac{\phi_0^2}{32\pi^2\lambda^2(0)H_{cb}^2(0)R^2}\left\{1+O\left[\left(\frac{d}{2R}\right)^4\right]\right\}. \quad (13)$$

In principle, phase diagrams of the type shown in Fig. 1(a) can be constructed from data obtained from isothermal, sample resistivity ρ-versus-magnetic-field H measurements. Figure 1(b) shows typical, expected ρ-versus-H curves for a series of successively lower temperatures, corresponding to the isotherms shown in Fig. 1(a).

III. REVIEW OF PREVIOUS EXPERIMENTAL WORK

The criterion which permits the construction of H_c-versus-T phase diagrams from isothermal H-versus-ρ data (discussed in Sec. II) is that the width of the resistive transition with field be smaller than the periodicity unit $(\Delta H)_{\min}=\phi_0/\pi R^2$ [from Eq. (11)], i.e.,

$$H(\rho=\rho_N,\ T)-H(\rho=0,\ T)\ll\phi_0/\pi R^2, \quad (14)$$

where ρ_N is the electrical resistivity of the hollow cylinder in the normal state. The experiments by Little and Parks did exhibit the predicted periodic behavior, but Eq. (14) was not satisfied. As a consequence, the ρ-versus-H curves were less ideal than those depicted in Fig. 1(b) [see Fig. 3(a)]. The oscillations in resistance were generally superimposed on a rather large parabolic background, which made it difficult to extract any information on the functional form of $H_c(T)$ beyond a precise determination of the field periodicity unit and order of magnitude estimates of the periodic oscillations in transition temperature, $(\Delta T_c)_{\max}$.[8,15] The origin of the parabolic background can be seen from a construction of the type shown in Fig. 2 (similar to the construction employed by Delmasso and Pagiola[10]), which is a ρ-H-T diagram for a sample with a rather broad resistive transition [i.e., a sample for which Eq. (14) is not satisfied]. Figure 2 was constructed by using Eq. (13) and assuming that the resistive transition (in zero field) is simply shifted under the application of field. The measured value of resistivity as a function of field at a given temperature, say, T_c, is found by the intersection of the plane perpendicular to the temperature axis at T_c and the ρ-H-T surface. Figure 3(b) is a plot of the expected ρ-versus-H dependence for the intersection at $T=T_c$ in Fig. 2. By comparing Fig. 3(b) with Fig. 3(a), it can be seen that the predicted observed effects are about the same order of magnitude. In the limit $\rho\to0$ (the H, T, $\rho=0$ plane), the quantum oscillations are superimposed on a parabolic background since the envelope curve [Eq. (8)] has a quadratic temperature dependence near T_c [i.e., $H_{\max}\propto(T_c-T)^{1/2}$]. Since the ρ-H-T surface was constructed by simply shifting the (assumed linear) ρ-versus-T curve in zero field, the intersection of the surface with a plane perpendicular to the T axis will yield a background curve $\rho\propto H^2$. Thus, even in the absence of the quantum periodicity, the ρ-versus-H curve should appear to have a quadratic form. This was found to be the case by Little and Parks, who did make a cylinder which was superconducting most of the way around and had a normal metal on the other part.[16] In the actual experimental situation, for a poor

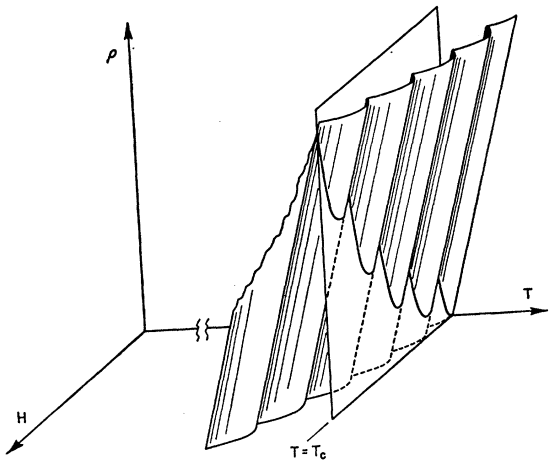

FIG. 2. ρ-H-T surface for a superconducting cylinder with finite wall thickness. The surface has been drawn assuming the zero-field resistance-versus-temperature curves to be undeformed under the application of field.

[14] C. J. Gorter and H. B. G. Casimir, Phys. Z. **35**, 963 (1934).

[15] L. Meyers and W. A. Little, Phys. Rev. Letters **13**, 325A (1964).

[16] See discussion following the paper by M. Tinkham, Rev. Mod. Phys. **36**, 268 (1964).

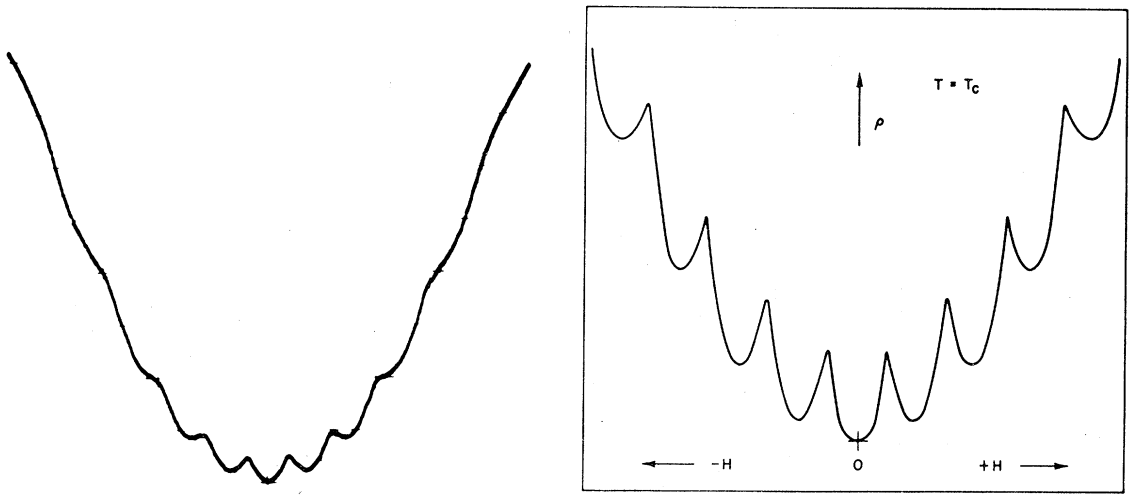

FIG. 3. (a) Oscilloscope trace of resistance versus magnetic field (from Ref. 8) for a tin cylinder. The abscissa is actual time, which was approximately proportional to the applied magnetic field. (b) Expected resistance-versus-magnetic-field behavior for the temperature $T=T_c$ in Fig. 2.

sample, the $\rho(H, T)$-versus-T curves are always deformed as shown in Fig. 4.

Parks and Little[8] obtained estimates of $(\Delta T_c)_{\max}$ by using the relation

$$(\Delta T_c)_{\max}\approx(\Delta\rho)_{\max}\Big/\left(\frac{\partial\rho}{\partial T}\right)_{H=0}, \tag{15}$$

where $(\partial\rho/\partial T)_{H=0}$ is the slope of the ρ-versus-T curve in zero field, and $(\Delta\rho)_{\max}$ is the maximum change in the periodic part of the sample resistance under applied field; that is, $(\Delta T_c)_{\max}$ was calculated assuming that the curves were not deformed under the application of field. Parks and Little determined $(\Delta T_c)_{\max}$ as a function of ρ/ρ_N, where ρ_N is the normal sample resistivity for a number of samples. In all cases reported, the apparent $(\Delta T_c)_{\max}$ found from Eq. (15) decreased monotonically with increasing ρ/ρ_N. This type of behavior can be accounted for by the same type of construction as mentioned in the preceding paragraph by incorporating the deformation[17] of $\rho(T)$ under H and taking the intersection of planes perpendicular to the T axis for successively higher values $T>T_c$ on the new ρ-H-T surface. This is equivalent to taking successively greater values of ρ/ρ_N. By so doing one obtains a calculated $(\Delta T_c)_{\max}$ which decreases montonically with increasing ρ/ρ_N. The calculations of Sec. II and the Appendices should be strictly valid only for infinitely sharp resistance transitions (and possibly the limit $\rho\rightarrow 0$) since no corrections were included to account for the finite breadth of the transition. A primary objective and accomplishment in the present work was to obtain samples which satisfied the suitability criterion given by Eq. (14), thereby allowing us to make comparisons between theory and experiment.

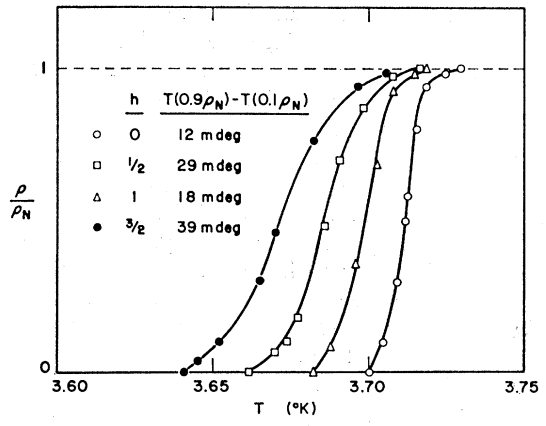

FIG. 4. Observed resistance-versus-temperature curves for four different values of the magnetic field for a low-quality tin cylinder of the present study.

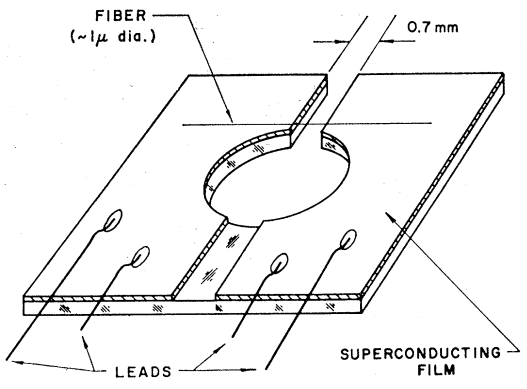

FIG. 5. Substrate arrangement for preparing microcylinders.

[17] Recall that the ρ-versus-T curves were drawn as being simply shifted with respect to $\rho(H=0, T)$ under the applied field when Fig. 3 was constructed.

IV. EXPERIMENTAL DETAILS

The necessarily small cylindrical substrates were prepared from GE-7031 insulating and dipping varnish, in essentially the same manner reported by Parks and Little.[8] The glue fibers were deposited on substrates fashioned from No. 2 or 3 cover glass slides as shown in Fig. 5. Small quartz fibers were tried in place of the varnish fibers for several samples. However, the superconducting transition temperatures for Al and Sn cylinders prepared on quartz fibers were generally 5–10% higher than the bulk values, and the resistive transitions were rather broad, suggesting that the films were severely strained.[18,19] Presumably the temperature coefficient of expansion of the glue is closer to the values for tin and aluminum than that of any of the other substrate materials tried. Also the quality of the quantization wiggles was generally not as good when other materials were used in place of the GE varnish. All of the samples used in the present study were deposited on glue fibers. One can estimate the diameter of the fibers to about 25% by observing the interference colors produced when the fibers are pulled. The earlier work[7,8] on extremely thin-walled cylinders had shown that the value of the diameter determined by the quantum periodicity condition [Eq. (10) with $d=0$ or Eq. (11)] agreed with the value obtained from electron-microscopy measurements to within 5%. Therefore, electron microscopy was not employed in this study and the cylinder diameters were determined directly from Eq. (11). Also, it should be mentioned that conventional optical microscopy is of little use in determining the fiber diameters (in the $\lesssim 1\ \mu$ range) because of the appearance of relatively large diffraction fringes.

The Al and Sn cylinders were prepared by metal coating the (suitably masked) fiber-holder assemblies (shown in Fig. 5) in a conventional liquid-nitrogen-trapped oil diffusion pump vacuum system. Pressures during the aluminum evaporations were maintained at $(1–3)\times10^{-7}$ Torr. Starting pressures for the tin evaporations were typically 2×10^{-6} Torr rising to $\sim(7–8)\times10^{-6}$ Torr during the evaporation. Unlike the case of aluminum, a relatively good vacuum was not essential for the preparation of good tin specimens. In fact, quite acceptable samples could be prepared in vacua approaching 10^{-3} Torr. Source-to-substrate distances were 20 cm. The substrates were rotated at 3 revolutions/sec during the evaporations. Deposition rates ranged from 50–90 Å/sec for aluminum and 80–150 Å/sec for tin. Film thicknesses were determined by multiple-beam interferometry using the method of fringes of equal chromatic order.[20] The problems of the rough surfaces of the tin specimens encountered previously[8] were largely overcome by evaporating the tin at a more rapid rate.

Four leads were attached to each sample with silver paint so that either two- or four-probe techniques could be used for monitoring the sample resistance. The samples were mounted with their axes along the axis of a superconducting solenoid and placed directly in the helium bath. Temperatures above 2.2°K were stabilized by a diaphragm manostat. Below the λ point of He^4, an electronic system was used. Allen Bradley $\frac{1}{8}$-W resistors in conjunction with a 100-cps Wheatstone Bridge, utilizing a phase-sensitive voltage amplifier as a null detector, were used for temperature measurement. During each run the resistors were calibrated against the vapor pressure of the helium bath. Since only relative temperatures were important in the experiment, hydrostatic corrections, etc., were neglected. The temperature sensitivity of this arrangement was better than 10^{-4} K°. The following method was used in taking ρ-versus-H measurements: The sample was placed in one arm of a Wheatstone Bridge operating at 27 cps (a two-probe technique was feasible because of the relatively large sample resistances). After amplification, the bridge output was fed into a phase-sensitive amplifier and into the Y axis of an X-Y recorder. The output of the amplifier was approximately linear with changes in the sample resistance. Lead and contact resistance were measured with the sample in the superconducting state. The sensitivity of this arrangement was $10^{-3}\ \Omega$ (with a bandwidth of $\sim$5 cps). This was the most convenient method for monitoring sample resistance, although both ac and dc four-probe techniques gave the same results. The largest measuring current to pass through any sample was less than 3×10^{-7} A (rms) which corresponds to a current density of less than 100 A/cm^2 for the smallest samples studied. The X axis of the recorder was used to monitor the current passing through the solenoid. Field sweep rates ranged from 0.005 to 0.5 G/sec, depending on the bandwidth of the amplifier.

V. EXPERIMENTAL RESULTS

A. Aluminum

Experimental ρ-versus-H curves at various representative temperatures for 1.33-μ-diam aluminum cylinder are shown in Fig. 6. The sample is completely superconducting at the minima, while the maxima correspond to the normal sample resistance. The same ρ-versus-H curves were obtained for both increasing and decreasing field sweeps. The slight slope of the normal resistance peaks was due in part to the response time of the measuring circuitry, although the field transition does have a finite breadth. Figure 7 shows the corresponding $H(T)$-versus-T phase diagram which was constructed by plotting the field values defining the half-width of the resistance peaks as a function of temperature. The wall thickness of all of the cylinders reported here was 2500 Å. The diameter was calculated

[18] J. M. Lock, Proc. Roy. Soc. (London) **A208**, 391 (1951).
[19] A. M. Toxen, Phys. Rev. **123**, 442 (1961).
[20] S. Tolansky, *Multiple Beam Interferometry of Surfaces and Films* (Clarendon Press, Oxford, England, 1948), 1st ed.

TABLE I. Summary of data on aluminum cylinders.

Sample	$2R$ (μ)	Periodic oscillations [Eq. (13)] $(\Delta T_c)_{max}$ (mdeg K)	$\lambda(0)$ (Å)	Envelope curve [Eq. (8)] $H_\parallel(0)$ (G)	$\lambda(0)$ (Å)	Resistivity [Eq. (A3)] $\lambda(0)$ (Å)
A	2.17	12	990	231	1170	1010
B	1.83	17	1075	218	1090	1010
C	1.68	20	1080	270	1360	1010
D	1.32	33	1070	220	1100	1010
E	1.20	40	1070	210	1060	1010

from Eq. (11), $(\Delta H)_{min}$ being the experimentally determined field increment separating temperature minima in the phase diagram. We shall treat the 1.33-μ cylinder as a representative sample in order to demonstrate how the quantities presented in Table I were obtained. The dashed line of Fig. 7 is the best fit of Eq. (8) through the local temperature maxima. Inserting the standard temperature dependence for $H_{cb}(T)$ and $\lambda(T)$ in Eq. (8) one finds $H_{||}(0)=220$ G. Using the value $H_{cb}(0)=100$ G [21] for the thermodynamic critical field at $T=0$, one obtains $\lambda(0)=1100$ Å. The value of $(\Delta T_c)_{max}$ was then measured from the envelope curve. For the sample under consideration $\Delta T_{c\,max}=33$ mdeg K. This value can be used in Eq. (13) to give $\lambda(0)=1070$ Å. The solid line in Fig. 7 is a plot of Eq. (12) using the value $\lambda(0)=1070$ Å. One final check can be made by computing $\lambda(0)$ from Eqs. (A3) and (A5). The transport mean free path may be expressed as

$$l=(\pi^2k^2/e^2)\,(1/\gamma v_f\rho_0), \tag{16}$$

where γ is the electronic specific-heat capacity in erg/cm^3 °K^2 and ρ_0 is the residual resistivity in emu.[22] The residual resistivities of all the aluminum samples studied were approximately 10^{-6} Ω cm. Using the free-electron values $\gamma_{Al}=1.37\times10^3$ erg/cm^3 °K^2 and $v_f=13.2\times10^7$ cm/sec,[23] one obtains $l=405$ Å for a residual resistivity of 1.0×10^{-6} Ω cm. Using Eqs. (A3), (A5), and (A6) with $\xi_{0Al}=16\,000$ Å and $\lambda_L=157$ Å,[24] one

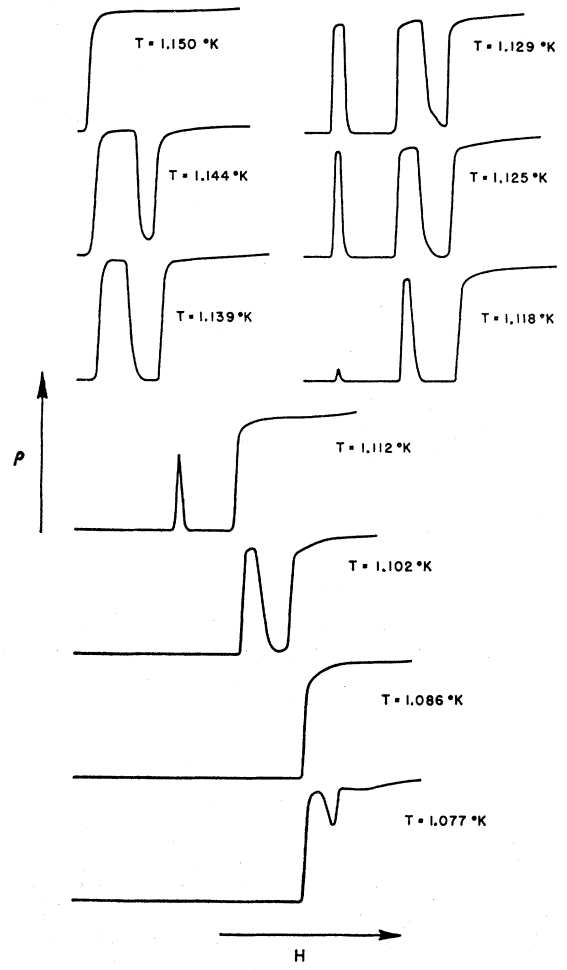

FIG. 6. Resistance-versus-magnetic-field curves (with temperature as a parameter) for a 1.33-μ-diam aluminum cylinder (sample D).

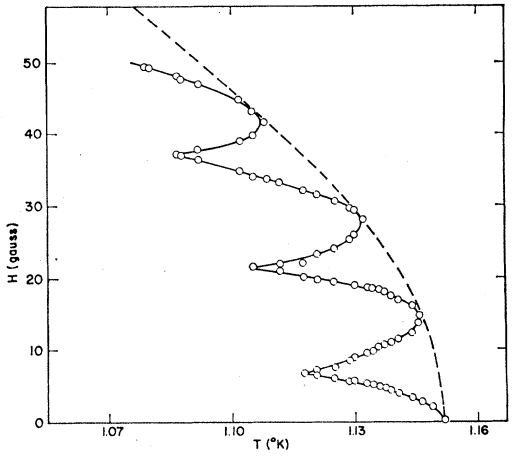

FIG. 7. Phase diagram for the 1.33-μ-diam cylinder. The diagram has been constructed from a number of isothermal resistance-versus-field measurements of which those in Fig. 10 are a characteristic few. The solid and dashed curves are explained in the text.

[21] B. W. Roberts, General Electric Research Laboratory Report No. 63-RL-3252M, 1963 (unpublished).
[22] B. B. Goodman, in *Metallic Solid Solutions*, edited by J. Friedel and A. Guinier (W. A. Benjamin, Inc., New York, 1963), p. 22.
[23] N. E. Phillips, Phys. Rev. Letters **3**, 17 (1959).
[24] J. Bardeen and J. R. Schrieffer, in *Progress in Low Temperature Physics*, edited by C. J. Gorter (North-Holland Publishing Co., Amsterdam, 1961), Vol. 3, p. 170.

obtains $\lambda(0)=1000$ Å, in good agreement with the two values found above.

In order to ensure that the agreement above was not due to a fortuitous choice of d and R, $(\Delta T_c)_{\max}$ was tabulated as a function of R for several samples of different radii. Figure 8 shows $(\Delta T_c)_{\max}$ versus $1/(2R)^2$ for the Al samples studied. As mentioned above, no corrections for differing mean-free-path effects were necessary. The slope of the solid line is

$$T_c\phi_0^2/8\pi^2\lambda^2(0)H_{cb}^2(0) \qquad (17)$$

with $\lambda(0)=1050$ Å, $T_c=1.2$°K, and $H_{cb}(0)=100$ G. The values of $\lambda(0)$ as determined from $H(0)$, $(\Delta T_c)_{\max}$, and resistivity are tabulated in Table I. Several cylinders of aluminum were made with diameters smaller than those presented here. However, the pumping capacity of the He^4 system was such that no data could be obtained below 1.08°K, which prohibited completing even one scallop on the $H_{||}(T)$-versus-T diagram for the cylinders of smaller diameter.

The aluminum films prepared in the manner described above all fall into the class of dirty superconductors, i.e., $l\ll\xi_0$, where ξ_0 is the bulk coherence length.

B. Tin

Because of the higher transition temperature of tin, one can obtain data for considerably smaller samples than was possible for aluminum. In fact, one is limited only by the ability to prepare sufficiently small cylindrical substrates. However, in many cases, the resistance-versus-field characteristics of the Sn samples have more rounded peaks than those of the Al samples. One particularly troublesome problem in the larger cylinders was an apparent "breaking up" of the cylinder into parallel "cigar-band"-like structures, each with a slightly different transition temperature and associated quantization oscillations. This effect can be quite troublesome in that it can lead to an apparent $(\Delta T_c)_{\max}$ much larger than really exists; i.e., the oscillations from two bandlike structures with only slightly different transition temperatures might tend to add. It was found that on samples of this type, one can sometimes work on the low-temperature end of the resistive transition, thus effectively looking at only the band with the lowest transition temperature. Many times this cannot be done, but when the last band to go superconducting on a poor sample can be isolated, the results are the same as for the better samples. The fields produced by diamagnetic screening currents from the totally superconducting bands should be negligible compared with the period $\Delta H_{\min}$ of the quantum oscillations ($\sim$0.1 G versus $\sim$3 G).

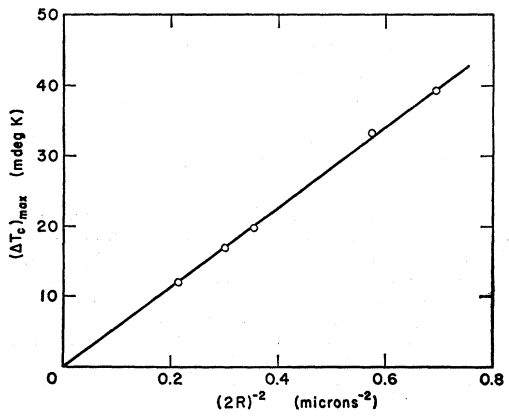

FIG. 8. Magnitude of the periodic oscillations $(\Delta T_c)_{\max}$ for the aluminum cylinders as a function of cylinder diameter $(2R)$.

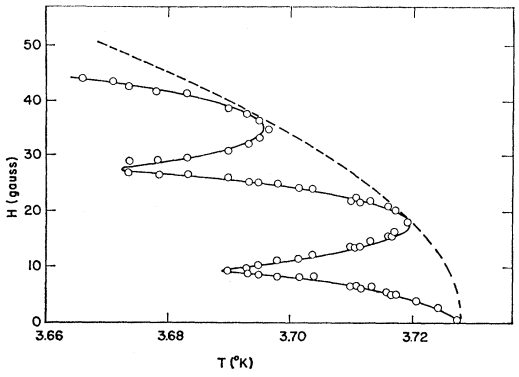

FIG. 9. Phase diagram for a 1.2-μ-diam tin cylinder (sample III). The solid line was calculated from Eq. (12) with $\lambda(0)=620$ Å, $T_c=3.73$°K, and $H_{cb}(0)=303$ G. The dashed curve is a "best fit" to Eq. (8) (see text).

Tin films prepared as described in Sec. IV typically exhibited room-temperature resistivities of $\sim 13\times10^{-6}\,\Omega$ cm. However, on occasion the measured room-temperature resistivity of a cylinder was found to be considerably higher than this value. This appears to be due to the tin cylinder's not making contact with the glass substrate at the edges rather than to some intrinsic effect (i.e., the effective length of the cylinder was greater than 0.7 mm). For this reason the resistivity ratio $\rho_{300°K}/\rho_{4.2°K}$ was used in estimating the residual resistivity for the samples, i.e.,

$$\rho_{4.2°K}\equiv(\rho_{4.2°K}/\rho_{300°K})_{\text{meas}}\times\rho_{\text{bulk}}. \qquad (18)$$

We shall choose the 1.2-μ cylinder of Fig. 9 as our representative sample. For this sample, $H_{||}(0)=390$ G. Using $H_{cb}(0)=303$ G [21] in Eq. (8), one obtains $\lambda(0)=617$ Å. The periodic deviations from the envelope curve (dashed curve in Fig. 9) gave a value $(\Delta T_c)_{\max}=37$ mdeg K, yielding $\lambda(0)=642$ Å from Eq. (13). If Eq. (16) is used with $v_f=6.5\times10^7$ cm/sec [24] and $\gamma_{Sn}=1.10\times10^3$ erg/cm^3 °K^2 (Ref. 25) obtains $\rho l=1.03\times10^{-11}\,\Omega$ cm^2 and $l_{\text{eff}}=2260$ Å for this sample. The resistivities of the tin samples used in this study were such that the mean free path was the same order of magnitude as the sample thickness. Previous work with tin foils seemed to indicate the presence of diffuse scattering of electrons at the surface.[26] If this is the

[25] E. A. Lynton, B. Serin, and M. Zucker, J. Phys. Chem. Solids **3**, 165 (1957).

[26] E. R. Andrew, Proc. Phys. Soc. (London) **A62**, 77 (1949).

TABLE II. Summary of data on tin cylinders.

Sample	$2R$ (μ)	Periodic oscillations [Eq. (13)] $(\Delta T_c)_{max}$ (mdeg K)	$\lambda(0)$ (Å)	Evelope curve [Eq. (8)] $H_\parallel(0)$ (G)	$\lambda(0)$ (Å)	Resistivity [Eq. (A3)] $\lambda(0)$ (Å)	
I	2.1	11.6	645	360	580	647	(612)
II	1.55	21	650	420	674	637	(592)
III	1.20	37	642	390	617	618	(581)
IV	1.35	30	635	380	620	628	(587)
V	1.17	27.6	760	500	800	667	(617)
VI	1.15	40.5	635	382	615	635	(590)
VII	1.08	45	645	415	670	655	(613)
VIII	0.92	70	600	355	575	662	(614)
IX	0.78	100	605	415	670	662	(614)
X	0.56	200	590	410	660	667	(617)

case the mean free path l_{eff} calculated in the above manner presumably corresponds to[27]

$$1/l_{eff}=1/l_{bulk}+\tfrac{3}{8}(1/d). \quad (19)$$

Therefore, ξ was determined from the relation

$$1/\xi=1/\xi_0+1/l_{eff} \quad (20)$$

rather than Eq. (A7).[28] Using $\xi_{0Sn}=2300$ Å, $\lambda_L=350$ Å,[20] and Eqs. (20) and (A3) together with the above values gives $\lambda(0)=618$ Å in good agreement (agreement better than $\pm 5\%$ is fortuitous) with the above values. The values of $\lambda(0)$ calculated from Eqs. (8), (13), and (A3) for the various samples are tabulated in Table II. Here we have chosen free-electron values for the calculation of l_{eff}. Chang and Serin[29] have determined that the value $\rho l=1.6\times10^{-11}$ Ω cm^2 was necessary to bring their measurements of κ_1 into agreement with theory. This higher value results in a slightly lower value of penetration depth calculated in the above manner. The calculated values of $\lambda(0)$ for $\rho l=1.6\times10^{-11}$ Ω cm^2 are shown in parentheses in the last column of Table II. Lyall and Cochran[30] obtain $\rho l=1.45\times10^{-11}$ Ω cm^2 for Sn from anomalous skin-effect measurements. Values of ρl obtained from both anomalous skin-effect studies and size-effect studies[31] on Sn range from 1.02×10^{-11} to 2.0×10^{-11} Ω cm^2.

In Fig. 10, we have plotted $(\Delta T_c)_{max}$ versus $(1/2R)^2$ for the Sn samples studied. No corrections were made for mean-free-path effects (i.e., different values of residual resistivities). The straight line is

$$\phi_0^2/8\pi^2\lambda^2(0)H_{cb}^2(0),$$

with $\lambda(0)=635$ Å, which corresponds to a resistivity ratio of 25. The value of $(\Delta T_c)_{max}$ seems to increase slowly as one goes to the smaller cylinder diameters. This effect appears to be rather small and therefore nothing more will be said about it.[32–35] Also shown in Fig. 10(b) are the samples reported by Parks and Little[8] (triangles) and one sample (sample V) from the present study (square) which had been deposited on a glass fiber. The solid triangles are data from Parks and Little for two Sn+1% In cylinders and the open triangles are for two Sn cylinders. The data of Parks and Little[8] were normalized in the following manner: First, the penetration depths $\lambda'(0)$ were calculated from quoted values of residual resistivity in the manner described above; and second, their reported value of $(\Delta T_c)_{max}$ [estimated from Eq. (15)] was multiplied by a factor λ'^2/λ^2, where $\lambda=635$ Å [the value of λ associated with the solid line of Fig. 10(b)] in order that these samples could be compared with the present work. The fact that $(\Delta T_c)_{max}$ for sample V was considerably smaller than $(\Delta T_c)_{max}$ for the tin samples prepared on varnish fibers illustrates the superiority of the 7031 varnish to glass (or quartz) as a substrate material for tin films [see also Sec. IV]. Further evidence for the inferiority of glass or quartz substrates is that sample V and other samples prepared on glass exhibited low quality ρ-versus-H characteristics.

The phase diagrams for several tin cylinders are shown in Fig. 11. These have been plotted with the same temperature and field scales so as to emphasize the dependence of $(\Delta T_c)_{max}$ on cylinder diameters.

[27] K. Fuchs, Proc. Cambridge Phil. Soc. **34**, 100 (1938).
[28] This should be a substantially better choice for ξ than Eq. (A7) because Eq. (A7) gives a surface-scattering event the same weight as a bulk-scattering event even though there are only the order $\frac{1}{3}$ of these for $l_{bulk}\sim d$.
[29] G. K. Chang and B. Serin, Phys. Rev. **145**, 274 (1966).
[30] K. R. Lyall and J. F. Cochran, Phys. Rev. **159**, 517 (1967).
[31] A review of the results of these studies is given in Ref. 30.
[32] If one uses the more sophisticated formalism due to Gor'kov (Ref. 33), Maki (Ref. 34), and de Gennes (Ref. 35) to solve for $(\Delta T_c)_{max}$, and includes terms to second order in $(\Delta T_c)_{max}$ and $(d/2R)^2$, then one gets a slight rise in the calculated value of $(\Delta T_c)_{max}$ as the cylinder diameter is decreased. However, for the range of cylinder diameters studied, this effect results in a less than 6% increase in the calculated value of $(\Delta T_c)_{max}(2R)^2$ which is less than the estimated experimental uncertainty.
[33] L. P. Gor'kov, Zh. Eksperim. i Teor. Fiz. **37**, 833 (1960) [English transl.: Soviet Phys.—JETP **10**, 593 (1960)].
[34] K. Maki, in *Low Temperature Physics*, edited by J. G. Duant *et al.* (Plenum Press, Inc., New York, 1965), Vol. 9, Part. A, p. 405.
[35] P. G. de Gennes, Physik Kondensierten Materie **3**, 79 (1964).

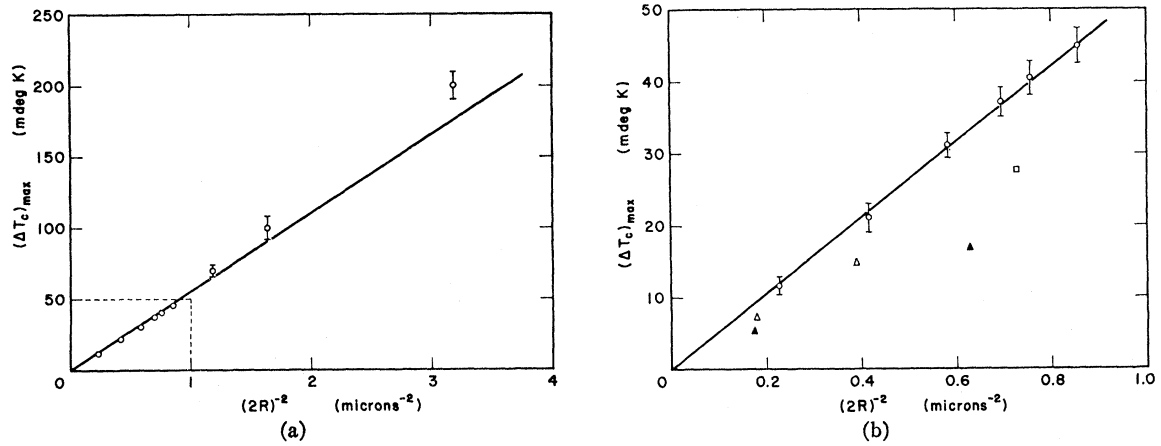

FIG. 10. (a) Magnitude of the periodic oscillations $(\Delta T_c)_{max}$ for the tin cylinders as a function of cylinder diameter $(2R)$. (b) Magnified display of the data in the vicinity of the origin in Fig. 10a. The triangles are the data of Parks and Little (see text) and the square is for a sample of the present study which was deposited on a glass substrate.

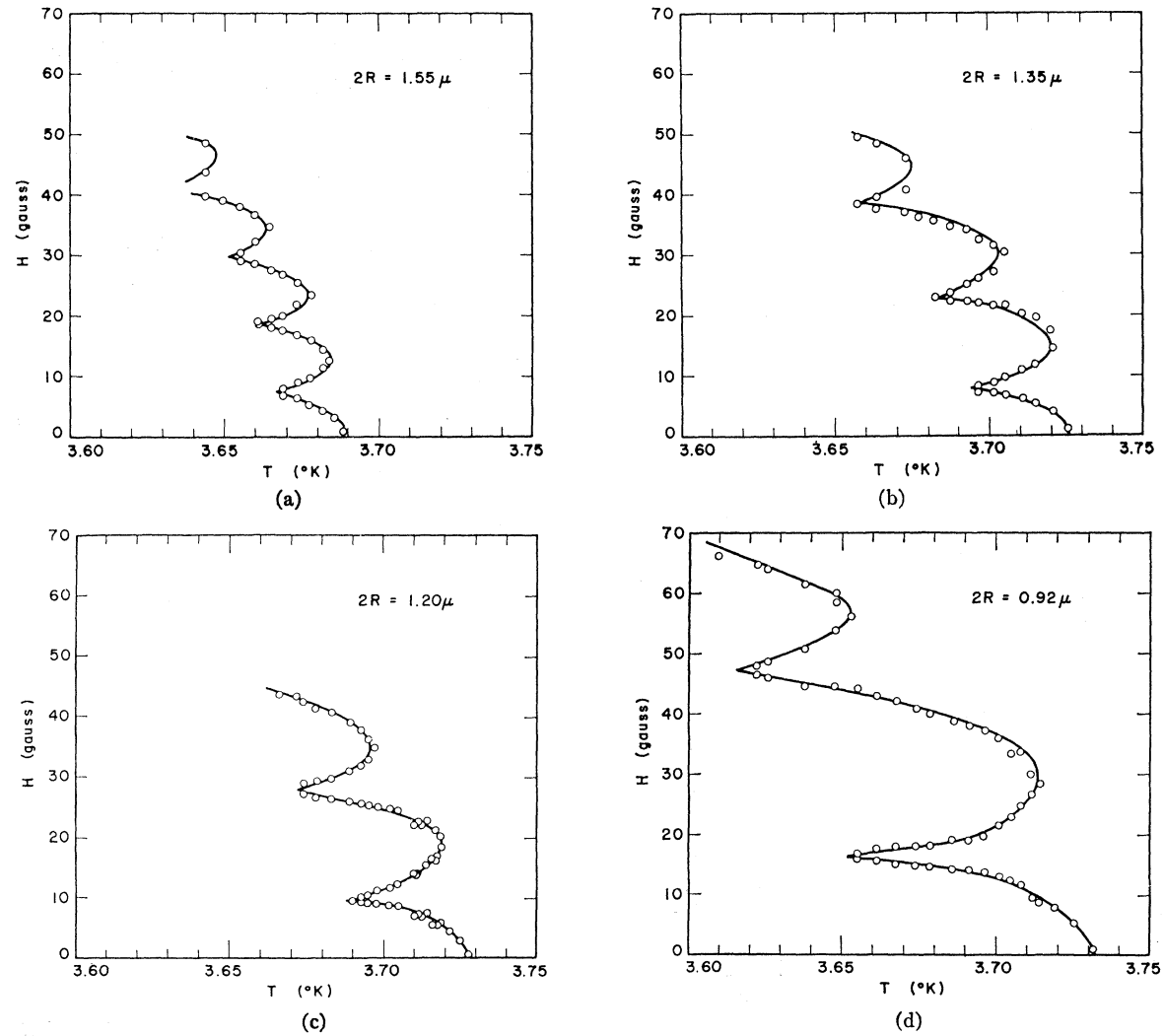

FIG. 11. Critical-field-versus-temperature curves for four tin cylinders of varying sizes. In each case the solid line was calculated from Eq. (12) with $H_{cb}(0)=303$ G and the following parameters: (a) $2R=1.55\ \mu$ (sample II), $\lambda(0)=650$ Å, $T_c=3.689$°K; (b) $2R=1.35\ \mu$ (sample IV), $\lambda(0)=625$ Å, $T_c=3.726$°K; (c) $2R=1.20\ \mu$ (sample III), $\lambda(0)=620$ Å, $T_c=3.728$°K; (d) $2R=0.92\ \mu$ (sample VIII), $\lambda(0)=575$ Å, $T_c=3.732$°K.

VI. DISCUSSION

We have measured the critical magnetic fields of thin hollow superconducting cylinders of tin and aluminum. By using improved samples we have essentially removed the parabolic background in the resistance-versus-field curves which plagued earlier work, thus making possible comparison of the quantitative aspects of theory with experiment. The experimental H_c-versus-T data are in quantitative agreement with predictions of the linearized Ginzburg-Landau equations in the immediate vicinity of T_c. However, as one gets farther from T_c the quantum oscillations tend to "wash out" sooner than the theory predicts. For example, consider Eqs. (6) and (9); one finds that the incremental field difference between a temperature maximum (associated with a given value of n) and an adjacent minimum (associated with the point common to n and $n-1$) decreases with increasing field (i.e., with increasing n). The field value at which a local minimum coincides with a local maximum is found by solving the equation

$$\frac{(n+1)}{1+(d/2R)^2}=\tfrac{1}{2}(2n+1)[1+\tfrac{1}{3}(d/2R)^2+\cdots]$$

for n, giving

$$n\leq\tfrac{3}{8}(2R/d)^2. \tag{21}$$

Thus for $(d/2R)^2>\frac{3}{8}$ one would expect no quantum oscillations to be present. The smallest Sn sample reported here (sample X) had $(d/2R)^2\approx 0.2$. For this particular sample, only one quantum oscillation was found and the resistance-versus-field curves were generally not as good as the others reported. In fact, several tin samples were run with diameters less than 0.5 μ (as determined from interference colors when preparing the substrates) and no quantum oscillations were found in any of them. Little time was spent on these extremely small diameter cylinders because, for the sample thicknesses involved, one was approaching the end of the range over which the superconducting transition was of second order [Eq. (4)]. For somewhat larger samples [e.g., the 1.2-μ-diam sample of Fig. 9 or Fig. 11(c)], one finds from Eq. (21) that it should be possible to observe seven to eight complete quantum oscillations. In actual practice, however, only about half that number could be observed before they completely washed out on resistance-versus-field plots. One possible explanation for this is nonuniformity of the cylinder diameters or the wall thickness.[36] Indeed, only a 6% variation in cylinder diameter along the length would be sufficient to reduce the total number of oscillations to three or four for a 1.2-μ-diam cylinder. We had no method of checking uniformity of cylinder diameter directly but the 6% variation implied by the point at which the quantum structure washes out is certainly quite reasonable. By taking sufficiently short samples it may be possible to obtain better agreement with the theory in this respect. Several attempts were made at preparing samples approximately 10 μ long. However, making good electrical contact to the cylinders proved to be an insurmountable obstacle.

[36] The possible importance of wall-thickness nonuniformity is discussed by R. Meservey and L. Meyers, Phys. Letters **26A**, 367 (1968).

VII. ANALYSIS OF EXPERIMENT WITHIN FRAMEWORK OF GENERAL DEPAIRING THEORY

Although the preceding sections treated the concept of fluxoid quantization as being primarily a critical field effect (because the critical field is the measurable quantity), a glance at Eq. (1) tells one immediately that it is the supercurrent density J that is responsible for the phenomenon. In this section it will be shown that the experiments discussed in the preceding sections provide a suitable method for studying current-induced second-order phase transitions in superconductors.

If the reduced energy gap parameter is written $\psi=fe^{i\eta}$, the current density Eq. (A2) can be written (see Appendix B)

$$J=\chi Ne(P/m)(1-P^2/P_d^2), \tag{22}$$

where $N=n_s\,|\,\Psi(T,0)\,|^2$ is the number of superconducting electrons in the absence of an applied field or current, $\mathbf{P}=\frac{1}{2}(\hbar\nabla\eta-(2e/c)\mathbf{A})$ is the "drift momentum" of the superconducting electrons, and

$$P_d=\omega_0(T)/v_f\chi^{1/2}, \tag{23}$$

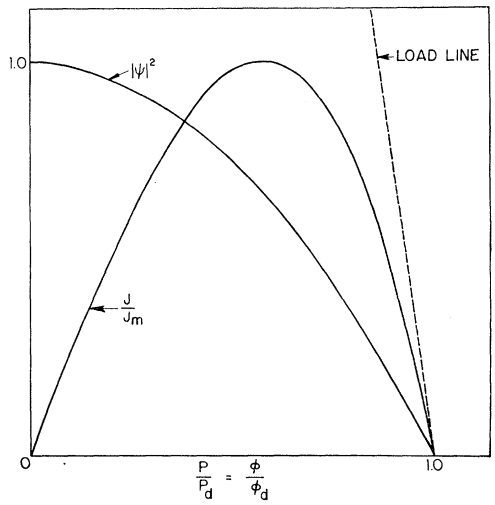

FIG. 12. Dependence of the order parameter ψ, and the current density J on the drift momentum of the superconducting electrons P. The straight line indicates a graphical solution of Eqs. (25) and (26). This load line has $\lambda^2/\mathrm{Rd}>1$, so that the entire region $P\leq P_d$ is accessible.

ω_0 being the temperature-dependent gap in the excitation spectrum. The quantities J and f^2 are plotted as a function of P in Fig. 12. The remarkable feature of the current-versus-momentum curve is the fact that the current density actually reaches a maximum at a momentum $P_m=P_d/\sqrt{3}$. As the (drift) momentum (or, alternatively, "drift" velocity) of the superconducting electrons is increased beyond P_m the supercurrent decreases monotonically to zero. The most important aspect of this (depairing) phenomenon is that it provides for a *gradual* loss of superconducting coherence[37] and leads finally to a second-order (since $f\to 0$ as $P\to P_d$) phase transition at $P=P_d$.

One can get a better idea of the physical significance of this phenomenon by considering its microscopic origin. The effect of a large Cooper-pair drift velocity ($\mathbf{v}=\mathbf{P}/m$) on the excitation spectrum of a superconductor was first considered by Bogoliubov.[13] In the framework of the BCS theory, the effect appears as a $\mathbf{p}_f\cdot\mathbf{v}_d$ term in the excitation spectrum, where $\mathbf{p}_f$ is the momentum of an electron at the Fermi surface.[38] When this added kinetic energy due to the drift velocity becomes comparable with the binding energy of the paired electrons, the Cooper pairs begin to become unstable with respect to individual quasiparticle excitations. The current density is then found to break up into two distinct parts,[39,40]

$$\mathbf{J}=\mathbf{J}_d+\mathbf{J}_{bf},$$

where $\mathbf{J}_d$ is proportional to $\mathbf{v}$ and $\mathbf{J}_{bf}$, called the "backflow current," results from the depairing process described above. Equation (23) agrees with microscopic calculations of P_d in the limits $T\to 0$ and $T\to T_c$ to within 5% for both the clean ($l\gg\xi_0$)[40] and dirty ($l\ll\xi_0$)[41] limits.

Now the question arises as to what portions of the J-versus-P curve (Fig. 12) can be explored in a critical current experiment. When a thin film (in particular, a compensated geometry which leads to a uniform current density in the sample) is used as a circuit element in series with a current generator, critical conditions are reached when the current density reaches its maximal value ($\partial J/\partial P=0$). If more than this amount of current is forced through the film ($J>J_m$), a sudden increase in the internal energy of the film takes place as the coherence is broken; i.e., the film undergoes a *first-order* transition to the normal state. Thus experiments in which the current is externally supplied cannot yield any information to the right of J_m in Fig. 12.

However, if an external agent can control P instead of J, it may be possible to obtain information about J to the right of J_m. P is determined by the geometry of the situation if the current is induced around a cylinder by means of an externally applied axial magnetic field. In this arrangement, since the electrons are inductively coupled to the driving force, J can increase and decrease at will, the only restriction being

$$P=\tfrac{1}{2}[\hbar n/r-(2e/c)A],$$

where we have used the fact from Appendix A that the order parameter must be single valued. The multiplicity of different states associated with the quantum number n complicates the situation; thus in the following we shall consider only the state with $n=0$. Also, in the interest of simplicity we assume f to be spatially constant [i.e., $d\ll\xi(T)$], so that the $\nabla^2 f$ terms in Eq. (A1) can be neglected.

Since $\oint\mathbf{A}\cdot d\mathbf{l}=\phi$, where ϕ is the flux threading the curve about which the integral is taken (in this case the cylinder), the momentum can be written

$$P=-(e/c)\phi/2\pi R. \tag{24}$$

The current density can now be expressed in terms of the flux threading the cylinder:

$$J=(\chi Ne/m)[-(e/c)(\phi/2\pi R)](1-\phi^2/\phi_d^2), \tag{25}$$

where ϕ_d is the flux necessary to produce a momentum P_d given by Eq. (23). The induced current density is then obtained from the simultaneous solutions of Eq. (25) and

$$\phi=\phi_{\text{ext}}+\mathfrak{L}dJ, \tag{26}$$

where $\mathfrak{L}=(4\pi^2/c)R^2$ is the inductance per unit length of the cylinder and ϕ_{ext} is the externally applied flux. Equations (25) and (26) are most conveniently solved graphically as indicated by the straight line in Fig. 12. The effect of increasing the external field can be visualized as a parallel translation of the load line so that its intersection with the abscissa is shifted to continuously larger values.[42] Clearly, if one is to explore the entire depairing regime the slope $(\mathfrak{L}d)^{-1}$ of the load line must be greater than the maximum slope of the current field characteristic, i.e., $(\mathfrak{L}d)^{-1}>\partial J/\partial\phi|_{\phi=\phi_d}$ or, using Eq. (A3),

$$\gamma=\lambda^2(T)/Rd>1. \tag{27}$$

This more stringent condition must replace the relation given by Eq. (4) as the criterion for a second-order phase transition. For $\gamma<1$, Douglass[4] finds that

[37] Electron tunneling measurements made on a thin superconductor in the regime $v_d\sim v(J=J_{\max})$ verified that the energy gap is somewhat depressed by the current. See J. L. Levine, Phys. Rev. Letters **15**, 154 (1965).

[38] Strictly speaking another term, $\frac{1}{2}mv_d^2$ should be added since the current carrying state is described by a slight displacement of the Fermi sphere in momentum space, i.e., $m\mathbf{v}_f\to m(\mathbf{v}_f+\mathbf{v}_d)$. Thus the expression that enters is

$$m(\mathbf{v}_f+\mathbf{v}_d)^2=p_f^2/2m+\mathbf{p}_f\cdot\mathbf{v}_d+\tfrac{1}{2}mv_d^2.$$

However, since $|\mathbf{v}_d|\ll|\mathbf{v}_f|$ this term is neglected.

[39] R. H. Parameter, RCA Rev. **26**, 323 (1962).

[40] K. T. Rogers, Ph.D. thesis, University of Illinois, 1960 (unpublished); also J. Bardeen, Rev. Mod. Phys. **34**, 667 (1962).

[41] K. Maki, Progr. Theoret. Phys. (Kyoto) **29**, 333 (1963).

[42] P. Fulde and R. A. Ferrell, Phys. Rev. **131**, 2457 (1963).

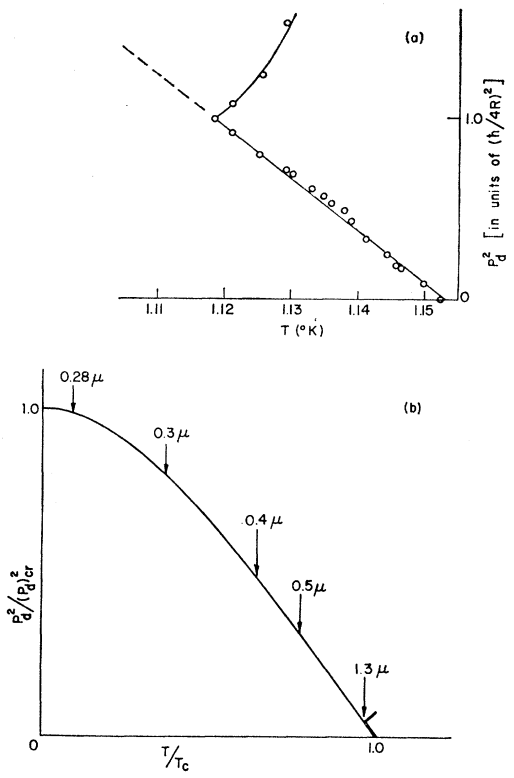

FIG. 13. (a) P^2 versus T for a 1.33-μ-diam aluminum cylinder (sample D). The dotted portion of the depairing curve is not accessible since the azimuthal quantum number n changes from 0 to 1 at $P_d=\hbar/4R$. (b) Generalized depairing curve. $(P_d)_{cr}$ is that value of P_d required to depress T_c to zero. The bold curve near T_c shows the portion of the depairing curve actually verified by the data of Fig. 13(a). The arrows mark the points on the depairing curve which can be reached with cylinders of different sizes.

$(\Delta T_c)_{\max}$ calculated on the basis of a second-order transition (as was done in Sec. II) should be diminished by the factor $(1+\gamma^2)/2\gamma$. This is not too serious in the range $\gamma \gtrsim \frac{1}{2}$ but can result in a severe degradation of the theoretical $(\Delta T_c)_{\max}$ for smaller values of γ. Unfortunately, for a given value of temperature the measured critical field in the present experiment yields only the value P_d. In order to retrace the whole portion of the J-versus-P curve to the right of J_m, one would have to measure accurately either the magnetization of the cylinder (which is extremely difficult) or the internal field of the cylinder (even more difficult). However, the temperature dependence of P_d is in itself quite interesting.

Ultimately, one would like to have a measure of P_d for all temperatures so that the generalized Ginzburg-Landau theory should be used.[43] For a second-order phase transition (the present case), critical conditions are determined by[44–46]

$$-\ln(T/T_c)=\psi_d[\tfrac{1}{2}+(\hbar\alpha/2\pi kT)]-\psi_d(\tfrac{1}{2}), \quad (28)$$

where T is the transition temperature in the presence of a pair-breaking force α, $T_c=\lim_{\alpha\to 0}T$, and ψ_d is the digamma function. The pair-breaking parameter α can be evaluated by solving the diffusion equation

$$-\tfrac{1}{6}(\tau v_f^2)[\nabla-(2ei/\hbar c)\mathbf{A}]^2\psi=\alpha\psi, \quad (29)$$

subject to the boundary conditions for the problem at hand. For the present case (thin hollow superconductor in an axial magnetic field), α takes the form

$$\langle\alpha\rangle=\tfrac{1}{6}(\tau v_f^2)\langle(1/r^2)(n-\pi r^2H/\phi_0)^2\rangle$$
$$=\tfrac{1}{6}(\tau v_F^2)(4\langle P_d^2\rangle/\hbar^2).$$

A spatial average has to be taken since we are not interested in local values of α. When this is done and $\langle\alpha\rangle$ is used in Eq. (28), the result is essentially the same as that obtained from the linearized Ginzburg-Landau equations for $T_c-T\ll T_c$ (Sec. II). Equations (28) and (29) are valid only in the dirty limit $l\ll\xi_0$ and hence should be applied only to the aluminum data. Figure 13(b) is a plot of the temperature dependence of P_d^2 (which is proportional to the pair-breaking parameter α).

Unfortunately, in the present study it was possible to test only a small portion of the P_d^2-versus-T curve, the limitation resulting from quantum switching effects. In this section we have implicitly assumed that $n=0$. However, when P_d reaches the value $P_d=\hbar/4R$, it becomes energetically favorable for the azimuthal quantum number n to change from 0 to 1. This has the consequence of keeping the drift momentum of the electrons (and hence $\langle\alpha\rangle$) small. The bold curve of Fig. 13(b) near T_c shows the portion of the total depairing curve that was verified with the 1.3-μ-diam aluminum cylinder. Figure 13(a) shows the agreement with the calculated values of P_d^2 on a greatly magnified scale. The arrows of Fig. 13(b) show cylinder diameters necessary to reach various portions of the depairing curve. For a given diameter cylinder, a correspondingly larger portion of the curve could be observed by simply increasing the electronic mean free path in the aluminum films. Increasing the mean free path of

[43] L. Tewordt, Phys. Rev. **137**, A1745 (1965).

[44] This equation was first derived by Abrikosov and Gor'kov (Ref. 45) in their treatment of depairing due to the presence of magnetic impurities, wherein α is proportional to the concentration of magnetic impurities. The equation has since been found to be applicable to a variety of other pair-breaking situations (see, e.g., Ref. 46).

[45] A. A. Abrikosov and L. P. Gor'kov, Zh. Eksperim. i Teor. Fiz. **39**, 1781 (1960) [English transl.: Soviet Phys.—JETP **12**, 1243 (1961)].

[46] K. Maki, in *Superconductivity*, edited by R. D. Parks (Marcel Dekker, Inc., New York, to be published).

aluminum from 400 to 1600 Å has the same effect as halving the cylinder diameter [the arrows in Fig. 13(b) are for a mean free path of 400 Å]. This can be done for aluminum without destroying the criterion ($l \ll \xi_0$) for applicability of the theory. However, due to the granular structure of aluminum films, this has not yet been possible.

Another difficulty which may become more serious in cylinders with sub-μ diameters is the fact that as one progresses further from the transition temperature, the criterion [Eq. (27)] for a second-order phase transition,

$$(\lambda^2(0)/Rd)[1/(1-t^4)]>1,$$

becomes harder to fulfill. Thus one would have to go to smaller film thicknesses in addition to the smaller cylinder diameters in order to ensure that the transition remain second order. This criterion was satisfied for all of the aluminum cylinders studied as well as the larger tin cylinders shown in Fig. 10(b). The three smallest tin cylinders did not satisfy Eq. (27) throughout the temperature range studied [although the less stringent condition of Eq. (4) was always satisfied]; i.e., at some temperature T_d such that $T_c - T_d < (\Delta T_c)_{\max}$, Eq. (27) ceased to be valid. However, at the temperature T_d where the transition becomes slightly first order, no change in the critical-field characteristics could be detected. In fact, the quantum periodicity in the critical field of all the tin cylinders studied persisted until γ reached a value somewhere between 0.4 and 0.6, depending on the particular sample. However, as we have already seen in Sec. VI, the point at which the quantum structure washes out can easily be accounted for by assuming a slight nonuniformity of cylinder diameter. Thus it seems likely that the point at which the quantum structure washes out is not connected with the order of the transition. As mentioned above, achieving sharp resistive transitions becomes more difficult as the film thickness is decreased. Another objection, possibly more serious, to decreasing either the diameter or wall thickness is that intrinsic thermodynamic fluctuations would tend to broaden the resistive transition and depress the transition temperature.[47–49]

APPENDIX A

For a hollow superconducting cylinder of arbitrary cross section in an axial magnetic field H, the Ginzburg-Landau[11] equations take the form

$$[\nabla - i(2e/\hbar c)\mathbf{A}]^2\psi + (\kappa^2/\lambda^2)(1-|\psi|^2)\psi = 0, \tag{A1}$$

$$(4\pi/c)\mathbf{J} = \nabla \times \nabla \times \mathbf{A} = (\hbar c/4ie\lambda^2)(\psi^*\nabla\psi - \psi\nabla\psi^*) - (|\psi|^2/\lambda^2)\mathbf{A} \tag{A2}$$

with boundary conditions

$$\nabla \times \mathbf{A} = \mathbf{H} \quad \text{on the outer surface,}$$

$$\nabla \times \mathbf{A} = 2\mathbf{A}/r \quad \text{on the inner surface,}$$

$$[\nabla\psi - (2ei/\hbar c)\mathbf{A}\psi]_r = 0 \quad \text{on both surfaces.}$$

We have assumed that the flux is continuous across the boundaries and that the field in the hole is constant with position.[4] Here $\mathbf{A}$ is the vector potential and the reduced energy gap parameter is $\psi = \Psi(T,\mathbf{A})/\Psi(T,0)$. The penetration depth λ and coupling constant κ are

$$\lambda^2 = \lambda_L^2(T)/\chi = mc^2/4\pi e^2 n_s |\Psi(T,0)|^2\chi, \tag{A3}$$

$$\kappa = \kappa_0/\chi = 2\sqrt{2}\pi\lambda_L^2(T)H_{cb}^2(T)/\phi_0\chi = 2\pi\sqrt{2}\lambda^2 H_{cb}(T)/\phi_0, \tag{A4}$$

where $H_{cb}(T)$ is the thermodynamic critical field. The function χ, which gives the modification of penetration depth due to collisions,[50] is

$$\chi(\rho) = [8/7\zeta(3)]\sum_{m=0}^{\infty}[(2m+1)^2(2m+1+\rho)]^{-1} = [8/7\zeta(3)]\rho^{-1}\{\tfrac{1}{8}\pi^2 + (2\rho)^{-1}[\psi_d(\tfrac{1}{2}) - \psi_d(\tfrac{1}{2}+\tfrac{1}{2}\rho)]\}, \tag{A5}$$

with

$$\rho = \hbar/2\pi\tau kT = 1.132(\xi_0/v_f\tau), \tag{A6}$$

where τ is the collision time, ξ_0 is the bulk coherence length, v_f is the Fermi velocity, ψ_d is the digamma function, and ζ is the Riemann zeta function.[51] For a film of thickness d, containing impurities of mean separation l_{bulk}, the collision rate may be expressed as[12,52]

$$1/\xi \equiv 1/v_f\tau = 1/\xi_0 + 1/l_{\text{bulk}} + 1/d. \tag{A7}$$

For $\rho \gg 1$,

$$\chi(\rho) \to \xi/\xi_0.$$

---

[47] R. P. Groff, S. Marcelja, W. E. Masker, and R. D. Parks, Phys. Rev. Letters **19**, 1328 (1967); R. D. Parks, in Proceedings of the Conference on Fluctuations in Superconductors, Monterrey, 1968 (unpublished).

[48] T. K. Hunt and J. E. Mercereau, Phys. Rev. Letters **18**, 551 (1967).

[49] W. W. Webb and R. J. Warburton, Phys. Rev. Letters **20**, 461 (1968).

[50] L. P. Gor'kov, Zh. Eksperim. i Teor. Fiz. **37**, 1407 (1959) [English transl.: Soviet Phys.—JETP **10**, 998 (1960)].

[51] A. Abramowitz and I. A. Stegun, *Handbook of Mathematical Functions* (National Bureau of Standards, Washington, D.C., 1964).

[52] M. Tinkham, Phys. Rev. **110**, 26 (1958).

For the present case, we shall write $\psi=fe^{i\eta}$. Consider the second Ginzburg-Landau equation [Eq. (A2)]. Assuming that the field is only in the axial direction, that no longitudinal current is flowing, and making use of the cylindrical symmetry one finds that $\eta=n\phi$ if the reduced gap parameter is to be single valued, where n is an integer and ϕ is the azimuthal angle. For films with $d<\xi_\Delta(t)$, where $\xi_\Delta(t)\approx[\xi_0\xi/(1-t)]^{1/2}$ is the characteristic length for variation of the gap parameter, f may be treated as spatially constant.[53] This condition was easily satisfied for all of the films reported in the study.

Using the above form for ψ and assuming its magnitude to be spatially constant, Eq. (A2) becomes a Bessel's equation which can be readily integrated, giving

$$A_\phi(r)=C_1I_1(rf/\lambda)+C_2K_1(rf/\lambda)+n\phi_0/2\pi r, \quad \text{(A8)}$$

where I_1 and K_1 are modified Bessel functions of the first kind.[51] The integration constants are readily found from the boundary conditions

$$C_1=\left(\left[K_1(\alpha)+\tfrac{1}{2}\alpha K_0(\alpha)\right]\frac{H\lambda}{f}-K_0(\beta)\,\frac{\phi_0 n}{2\pi(R_m-\frac{1}{2}d)}\right)\Big/\,\Gamma,$$

$$C_2=\left(\left[\tfrac{1}{2}\alpha I_0(\alpha)-I_1(\alpha)\right]\frac{H\lambda}{f}-I_0(\beta)\,\frac{\phi_0 n}{2\pi(R_m-\frac{1}{2}d)}\right)\Big/\,\Gamma,$$

with

$$\Gamma=I_0(\beta)\left[K_1(\alpha)+\tfrac{1}{2}\alpha K_0(\alpha)\right]+K_0(\beta)\left[I_1(\alpha)-\tfrac{1}{2}\alpha I_0(\alpha)\right],$$

$$\alpha=(R_m-\tfrac{1}{2}d)f/\lambda, \qquad \beta=(R_m+\tfrac{1}{2}d)f/\lambda,$$

and R_m is the mean radius of the cylinder.

The present study was concerned primarily with second-order transitions. Therefore, we consider only the limiting form $f\to 0$ for A since this defines the transition to the normal state. This results in the more familiar expression

$$\lim_{f\to 0}A_\phi=\tfrac{1}{2}rH.$$

An expression for the transition temperature of the superconducting cylinder can now be obtained by substituting the limiting expression for A_ϕ into Eq. (A1) and averaging over the volume of the superconductor:

$$\frac{\kappa^2}{\lambda^2}=\frac{2e}{\hbar c}\left[(dR_m)^{-1}\int_{R_m-d/2}^{R_m+d/2}r\left(\tfrac{1}{2}rH-\frac{\hbar c}{2e}\frac{n}{r}\right)^2dr\right].$$

The result is given as Eq. (5). This result differs slightly from that of Douglass (because of an error in the expansion of the vector potential in Ref. 4) but agrees with that obtained by Delmasso and Pagiola[10] in a slightly different approximation.

APPENDIX B

As in Appendix A, if the reduced energy gap parameter is written $\psi=fe^{i\eta}$, Eq. (A2) becomes with the help of Eq. (A3)

$$\mathbf{J}=\chi f^2 n_s|\Psi(T,0)|^2(e/2m)[\hbar\nabla\eta-(2e/c)\mathbf{A}]. \quad \text{(B1)}$$

Recalling that $f^2=|\Psi(T,A)|^2/|\Psi(T,0)|^2$, the quantity $N=n_sf^2|\Psi(T,0)|^2$ just gives the total number of superconducting electrons in an applied magnetic field. Our expression for $\mathbf{J}$ then takes the form

$$\mathbf{J}=\chi Ne[(\hbar\nabla\eta-(2e/c)\mathbf{A})/2m],$$

so it becomes quite natural to assume the quantity

$$\hbar\nabla\eta-(2e/c)\mathbf{A}$$

to be the drift momentum of a Cooper pair of mass $2m$. If f is spatially constant (i.e., $d<\xi_\Delta$), Eq. (A1) can be written

$$f^2=1-P^2/P_d^2, \quad \text{(B2)}$$

where P is the drift momentum of a single superconducting electron (taken for simplicity to be one-half that of a Cooper pair) and the quantity P_d is given by

$$P_d^2=\hbar^2\kappa^2/4\lambda^2.$$

Using the standard temperature dependences[14] for κ and λ, and the BCS relation[6]

$$H_{cb}^2(0)=4\pi[\tfrac{3}{2}(n_s/mv_f^2)]\omega_0^2(0),$$

where $\omega_0(0)$ is the gap in the excitation spectrum at $T=0°\text{K}$, one obtains

$$P_d^2=\frac{3\omega_0^2(0)}{\chi v_f^2}\,\frac{T_c-T}{T_c}. \quad \text{(B3)}$$

The above expansion is restricted to the region $T_c-T\ll T_c$. In order to obtain a more useful criterion for going to lower temperatures, one can make use of the relation[54]

$$\omega_0^2(T)/\omega_0^2(0)\approx 3(T_c-T)/T_c \quad \text{for} \quad T_c-T\ll T_c.$$

The result is given as Eq. (23).

[53] P. G. De Gennes and M. Tinkham, Physics **1**, 107 (1964).

[54] R. A. Ferrell, Z. Physik **182**, 1 (1964).